

Computational design and optimization of quad meshes based on diagonal meshes

Caigui Jiang¹, Cheng Wang¹, Eike Schling², Helmut Pottmann¹

¹ Visual Computing Center

King Abdullah University of Science and Technology, Thuwal 23955, Saudi Arabia
caigui.jiang@kaust.edu.sa

² Department of Architecture

The University of Hong Kong, Knowles Building, Pokfulam Road, Hong Kong
schling@hku.hk

Abstract

A significant amount of research in Architectural Geometry has dealt with skins and structures which follow a quadrilateral layout with double curvature. In many cases, such quad networks are computationally accessed by quad meshes which obey various constraints. These may concern planarity of faces, supporting structures which follow specific curvature paths, conditions on node angles, static equilibrium and others.

In this paper we draw the attention to a new way of computing such constrained quad meshes. The new methodology is based on the diagonal meshes of a quad mesh and the checkerboard pattern of parallelograms one obtains by subdividing a quad mesh at its edge midpoints. The new approach is easy to understand and implement. It simplifies the transfer from the familiar theory of smooth surfaces to the discrete setting of quad meshes. This is illustrated with planar quad meshes and asymptotic nets, in particular with those exhibiting a constant node angle.

The application of such networks has advanced fabrication-aware-design in the architectural practice. Looking at asymptotic nets specifically, we list their potentials and challenges for the construction of strained gridshells. The benefits of constant node angles are highlighted along different construction methods in timber and steel. We conclude with current developments, looking at less-restricted and transformable asymptotic structures, and how they are designed.

Keywords: Quad meshes, mesh optimization, constrained meshes, asymptotic curves, construction-aware design, gridshells

1 Introduction

Architectural skins are frequently based on quadrilateral meshes which are aligned with panel boundaries and the support structure. Various construction constraints lead to specific types of underlying quad meshes. This has been a topic of numerous papers on architectural geometry. For an overview, we refer to Pottmann et al. (2015). The most prominent examples are meshes with planar quads (PQ meshes), in particular those whose panels are nearly rectangular. Those “principal meshes” enjoy a number of favorable properties for architectural applications, but they are also important from a purely geometric perspective (see Liu et al. (2006); Pottmann et al. (2007); Bobenko and Suris (2008)). Geometrically speaking, they follow the principal curvature lines of an underlying smooth reference surface.

Another important type of meshes, which however only exist on surfaces with negative Gaussian curvature, are asymptotic meshes or A-nets. These are quad meshes with planar vertex stars, i.e., a vertex and its four connected neighbors lie in a plane (see Bobenko and Suris (2008)). Such meshes follow the asymptotic curves (curves with vanishing normal curvature) of a smooth reference surface. They form the basis of asymptotic gridshells, which can be manufactured from planar straight metal strips (Schling (2018); Schling et al. (2018); see Fig. 1).

In this paper we would like to draw the attention to a new way of computing such constrained quad meshes. The new methodology is based on the diagonal meshes of a quad mesh and emerged in work of Jiang et al. (2019) on certain checkerboard patterns of rectangles which approximate surfaces. It is easier to deal with than previous methods, especially from a computational perspective. Moreover, it allows one to transfer certain concepts from the classical setting of smooth surfaces to quad meshes in a rather straightforward way.

In particular we deal with discrete intersection angles, called *node angles*, which we understand in the following sense: A fair quad mesh can be seen as a discrete version of a network of curves on a smooth surface. The network curves intersect each other at an angle which may or may not depend on the location. Here, we mostly deal with the latter case of a constant angle. For example, the network of principal curvature lines on a surface has a right intersection angle. Discrete versions of it are the principal meshes mentioned above. We will call them PQ meshes with a right node angle, which is meant as a discrete counterpart of the smooth setting. In fact, for a conical or circular mesh, usually none of the four edges meeting at a vertex (node) will do so under right angle. However, under refinement and by keeping the defining property, the mesh will converge to an orthogonal curve network, namely the principal curvature lines. In the present paper, we will study other node angles than right ones as well. Finding proper discrete expressions has not been easy with previous approaches, but is very simple with the present technique.

Finally, we look at the application of such meshes in architecture. Focusing on asymptotic networks we discuss the benefits of constant node angles along different

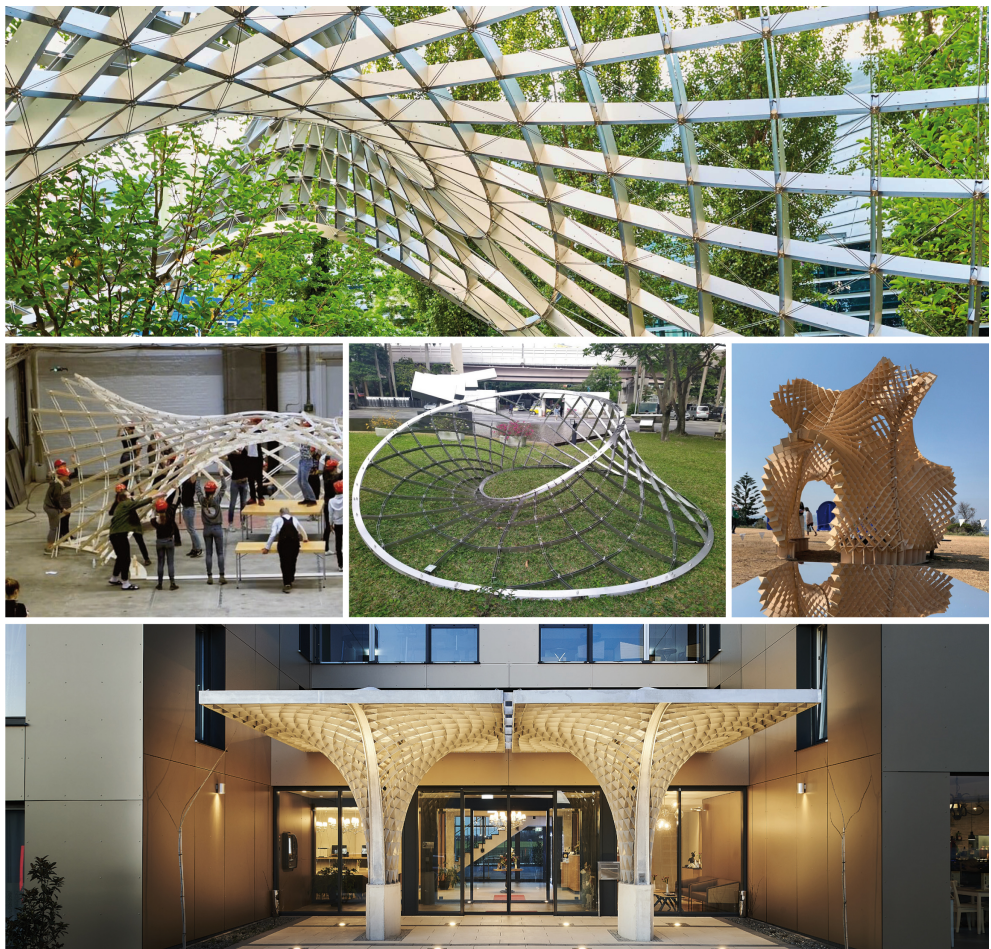


Figure 1: Asymptotic Gridshells have enjoyed international popularity in academic and commercial projects. Top Row: INSIDE/OUT Pavilion at the TUM Campus in Munich (Schling et al. (2017)). Second Row: Left: Workshops at Chalmers University in Gothenburg (2019 and 2020) (Adiels et al. (2019)); Middle: Steel Structure at the National Taiwan University of Science and Technology (Shih et al. (2019)); Right: Super Succah, Sculpture at the Sea, Bondi, Sydney (Maxwell (2019)). Bottom Row: First permanent Asymptotic Canopy for the Intergroup Hotel in Ingolstadt in collaboration with Brandl Steel, Eitensheim (Schling and Schikore (2020)).

construction methods in timber and steel. Node angles may also be used as design parameters. We introduce recent and future projects with variable node-angles that create freeform and transformable asymptotic structures.

1.1 Overview and contributions

- We provide alternative discrete models for quad meshes which are of interest in architecture. Our approach uses the two diagonal meshes of a quad mesh (*control mesh*) and a checkerboard pattern of parallelograms which arises from the control mesh by subdivision at edge midpoints.
- We show how to design and optimize PQ meshes and A-nets with a specific focus on controlling the node angle. In particular, we discuss PQ meshes with a constant node angle that needs not be a right angle. Among these structures, we find checkerboard patterns from “white” planar faces and “black” rhombi which are similar to each other (scaled versions of each other). They appear as a discrete model of a class of surfaces which extends the well-known isothermic surfaces. The latter can be represented by checkerboard patterns from black squares and white planar faces.
- We discuss A-nets with a constant node angle, thereby simplifying a recent approach by Jimenez et al. (2020).
- We show how to solve rationalization problems with the structures mentioned above.
- We use the node angle as a design tool in form-finding processes.
- We illustrate our work by real projects and fabricated models.

1.2 Related work

The idea of checkerboard patterns and the closely related concept of working with a pair of meshes previously appeared in various special cases in pure mathematics. Kenyon (2002) uses it in connection with discrete complex analysis, while Bobenko et al. (2016) and Techter (2020) employ mesh pairs to express right angles for discrete versions of the orthogonal system of confocal quadrics.

Following up on checkerboard patterns by Jiang et al. (2019), Jiang et al. (2020) present a new approach to discrete developable surfaces and isometric deformations, a topic which is also of high interest in architecture. The discrete developable surfaces therein are more flexible than previous versions, among which the discrete orthogonal geodesic nets by Rabinovich et al. (2018) are probably the most interesting ones.

The optimization framework which we employ in our research is not considered a contribution, as we simply follow Tang et al. (2014) and Jiang et al. (2019).

2 Theory and computation

General setup. Our structures are derived from a quad mesh C , called *control mesh*. Inserting edge midpoints in a not necessarily planar quadrilateral and connecting

them, one obtains a parallelogram (Fig.2, left). By the intercept theorem, its edges are parallel to the diagonals of the quad and have half their length. Performing this mid-edge subdivision in all quads of C , we obtain a checkerboard (CB) pattern P with one family of planar quads (we call them the black ones) being parallelograms (Fig.2, middle). The other (white) quads are in general not planar, but they are scaled versions with factor $1/2$ of a face in one of the two diagonal meshes D_1, D_2 of C (Fig. 2, right; and Fig. 11, middle).

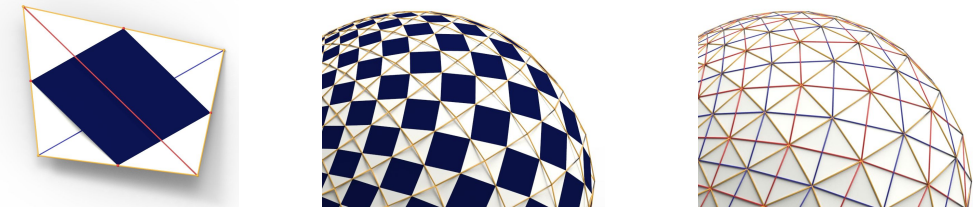


Figure 2: Left: The edge midpoints of a quad form the vertices of a parallelogram whose edges are parallel to the diagonals of the quad and of half their length. Middle: These parallelograms form a checkerboard pattern. Right: The diagonals of a quad mesh (yellow) can be arranged in two quad meshes (red, blue). Each white face in the checkerboard pattern is a scaled version (with factor $1/2$) of a face in one of the two diagonal meshes.

As discussed in more detail by Jiang et al. (2019), the black parallelograms provide first order information on the discrete surface parameterization which is represented by the pattern P , and in fact also by both of the diagonal meshes D_1, D_2 . For example, if the parallelograms are rectangles, P and D_1, D_2 can be considered as discrete orthogonal nets.

A key observation is the following one: Node angles measure discrete intersection angles of mesh polylines. In each quad of the control mesh, the two edges of the mesh pair (D_1, D_2) are the diagonals of that quad. They may be seen as discrete surface tangents and their angle is easily computed. Hence, *in our discrete model node angles appear as angles between diagonals in the quads of the control mesh*.

Planar quads and constant angle. If we want a CB-pattern from planar quads, we also have to make the white faces planar. This implies that both diagonal meshes D_1, D_2 have to be PQ meshes. So far, there is no advantage of using two meshes. However, it becomes apparent if want the planar quads to be as rectangular as possible. Then, all parallelograms in the pattern P have to be rectangles. This is expressed via the additional constraint that each quad of the control mesh C has to possess orthogonal diagonals. Note that this condition is simpler than the ones involved in circular meshes or conical meshes which have been used previously to obtain PQ meshes whose faces are as rectangular as possible (principal meshes). While the CB-pattern itself lacks a bit in terms of smoothness, each of the two diagonal meshes is a principal mesh, with all advantages that come with it, e.g., the existence of a torsion free support structure (see also Jiang et al. (2019)). The node axes of the support structure are easily computed. The axes for the vertices of



Figure 3: Principal meshes in the diagonal mesh approach have discrete surface normals which are suitable as node axes of a torsion free support structure. Left: The node axis at a vertex of one diagonal mesh (red) is orthogonal to the corresponding planar face of the other diagonal mesh (blue). Hence, node axes at connected vertices lie in the normal plane of the orthogonal crossing diagonal (blue). Right: Torsion free support structure attached to a principal diagonal mesh.

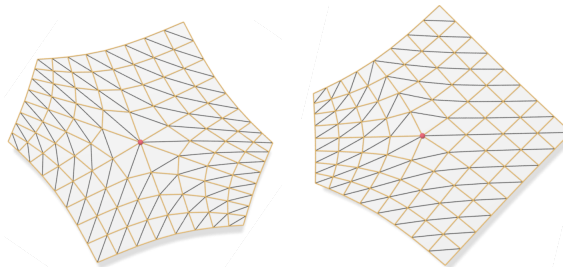


Figure 4: The angle between two diagonals can be determined by the rotation from one diagonal (black) to the other. This requires the selection of one diagonal per quad so that they form fair polylines, which is only possible for even valence v (left, $v = 6$), but fails for odd valence (right, $v = 5$).

D_1 are orthogonal to the corresponding faces in D_2 , and vice versa (see Figure 10).

It is easy to change the constant angle from a right one to another angle α . The angle is reflected in the angle of the diagonals in the quads of the control mesh. The only issue with a constant angle $\alpha \neq \pi/2$ is that one has to prescribe which of the two angles is α in which is $\pi - \alpha$. To do this, we select one diagonal in each quad and call it $\mathbf{v}_{i0}\mathbf{v}_{i2}$. The other diagonal is then $\mathbf{v}_{i1}\mathbf{v}_{i3}$, assuming that the vertices occur in the order $\mathbf{v}_{i0}, \dots, \mathbf{v}_{i3}$ in a counterclockwise orientation, when viewed from one selected side of the surface (Fig. 11, left). The angle α is then enforced between vectors $\mathbf{v}_{i2} - \mathbf{v}_{i0}$ and $\mathbf{v}_{i3} - \mathbf{v}_{i1}$ (see Equation (4)). To obtain a visually smooth result, this requires a choice of diagonals per quad so that these diagonals form fair polylines. At combinatorial singularities of the mesh this is only possible if an even number of edges meets there (Fig. 4). Hence, we can only work with control meshes whose singularities are of even valence.

A CB-pattern associated with these PQ meshes and a constant angle is formed by parallelograms all of which have the inner angles α and $\pi - \alpha$. One can even further restrict these meshes and require that all these parallelograms are *rhombs*, i.e., have equal edge length. But the edge length varies over the structure. To achieve this, we just have to make sure that the two diagonals in each quad of C have the same length. For a right angle, we obtain checkerboard patterns of congruent black squares and white planar faces. It has been argued by Jiang et al. (2019) that these are discrete isothermic surfaces and as such subject to a shape restriction of

the reference shape. The case of similar rhombuses (not squares; see Fig. 12) also has a counterpart in the smooth theory: These are conjugate parameterizations which can be mapped conformally to a planar grid of parallel lines with constant angle α . We are not aware of a study of such surfaces in differential geometry.

For *rationalization* of a given design surface with a PQ mesh of a constant node angle α in the above sense, one first has to investigate the smooth setting. A PQ mesh is a discrete counterpart of a so-called conjugate curve network. At each point, the two curves of the network are tangent to conjugate directions. Conjugate directions are a second order concept and depend on the curvature behavior. To understand it, we may introduce a local Cartesian coordinate system in the tangent plane at a point p of a surface S , whose axes are the two principal directions. Denoting the associated principal curvatures by κ_1, κ_2 , the normal curvature κ_n in a tangent direction $t = (\cos\phi, \sin\phi)$ at angle ϕ against the first principal direction is computed via Euler's formula:

$$\kappa_n = \kappa_1 \cos^2 \phi + \kappa_2 \sin^2 \phi. \quad (1)$$

In this local system, conjugate directions $t_1 = (x_1, y_1)$ and $t_2 = (x_2, y_2)$ are characterized by

$$\kappa_1 x_1 x_2 + \kappa_2 y_1 y_2 = 0. \quad (2)$$

Our PQ meshes of constant angle are discrete versions of conjugate networks with constant angle. Hence, we have to look for those pairs of conjugate directions at a surface point which form the angle α . For $\alpha = \pi/2$, these are the principal directions ((1,0) and (0,1)). For another angle α , we have to find a pair of directions $t_1 = (\cos\phi, \sin\phi)$ and $t_2 = (\cos(\phi+\alpha), \sin(\phi+\alpha))$ which satisfy (2). We obtain the condition

$$(\kappa_2 - \kappa_1) \cos(2\phi + \alpha) = (\kappa_1 + \kappa_2) \cos\alpha. \quad (3)$$

For our application, the angle α is given and ϕ is computed,

$$\phi = (\arccos C - \alpha)/2, \quad C = \frac{\kappa_1 + \kappa_2}{\kappa_2 - \kappa_1} \cos\alpha.$$

This requires $-1 \leq C \leq 1$. Due to the symmetry with respect to the principal curvature directions, a solution pair to (ϕ, α) implies the symmetric solution pair to angles $(-\phi, -\alpha)$. Depending on the sign of the Gaussian curvature $K = \kappa_1 \kappa_2$, we have the following three cases.

- $K < 0$, hyperbolic surface point. There, we have two solution pairs for any choice of α . It includes the limit case of asymptotic directions ($\tan\phi = \sqrt{|\kappa_1/\kappa_2|}$), which are characterized by vanishing normal curvature, are self conjugate and thus belong to $\alpha = 0$.
- $K = 0$, parabolic surface point. Let us assume $\kappa_1 = 0, \kappa_2 \neq 0$. Now (3) reads $\cos(2\phi + \alpha) = \cos\alpha$ and shows that $\phi = 0$ yields a solution for any α . This expresses that fact that any direction is conjugate to the single asymptotic direction (1,0).

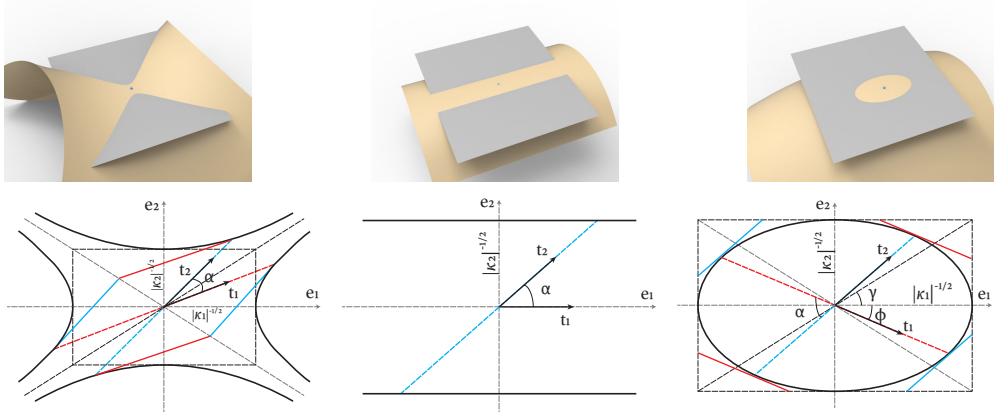


Figure 5: Top: The indicatrix at a point p may be obtained by intersecting the surface with planes parallel to the tangent plane at p . If the cutting plane approaches the tangent plane (for $K < 0$ (left) from both sides) and the intersection gets magnified appropriately, the limit curve is the indicatrix. *Bottom:* The indicatrix is a pair of hyperbolas for $K < 0$ (left), a pair of parallel lines for $K = 0$ (middle) and an ellipse for $K > 0$ (right). Conjugate directions t_1, t_2 belong to conjugate diameters of the indicatrix. For $K = 0$, conjugacy degenerates and any direction is conjugate to the asymptotic direction t_1 . For $K > 0$ (right), the conjugate directions with the smallest angle are the diagonals of the axis rectangle (characteristic directions).

- $K > 0$, elliptic surface point. In this case, we only have a certain interval for possible values of α , namely $\alpha \in [2\gamma, \pi/2]$, with $\tan \gamma = \sqrt{\kappa_1/\kappa_2}$. Here, γ is the angle of a so-called *characteristic direction* against the first principal direction (Fig. 5, bottom right). Its conjugate direction is symmetric with respect to the principal directions. This interval for α reduces to the single value $\alpha = \pi/2$ (i.e., $\gamma = \pi/4$) at an umbilic ($\kappa_1 = \kappa_2$), where any two conjugate directions are orthogonal.

A visualization of the behavior of conjugate directions can be based on the so-called *Dupin indicatrix*. This is a radial curvature diagram in the tangent plane at a surface point p . In the principal frame it is given by $(r(\phi)\cos\phi, r(\phi)\sin\phi)$ with the radial distance $r(\phi) = 1/\sqrt{|\kappa_n(\phi)|}$. Of course, the normal curvature $\kappa_n(\phi)$ follows Euler's formula (1), from which one concludes that the indicatrix has an equation of the form $\kappa_1 x^2 + \kappa_2 y^2 = \pm 1$. It is a pair of hyperbolas for $K < 0$, a pair of parallel lines for $K = 0$ and an ellipse for $K > 0$ (see Fig. 5, bottom). The case $K = 0$ is degenerate; all directions are conjugate to the principal direction with normal curvature $\kappa_1 = 0$. In the other cases, conjugate directions are given by conjugate diameters of the indicatrix: The tangents at the endpoints of one diameter are parallel to the other diameter. The tangents at the vertices $(\pm 1/\sqrt{|\kappa_1|}, 0)$ and $(0, \pm 1/\sqrt{|\kappa_2|})$ of the indicatrix form the axis rectangle. The diagonals of the axis rectangle are the asymptotic directions for $K < 0$ and the characteristic directions for $K > 0$ (Fig. 5).

Rationalization can now proceed as follows (see Fig. 6): Given a reference surface S , we compute a field of tangential frames (pairs of conjugate directions with angle

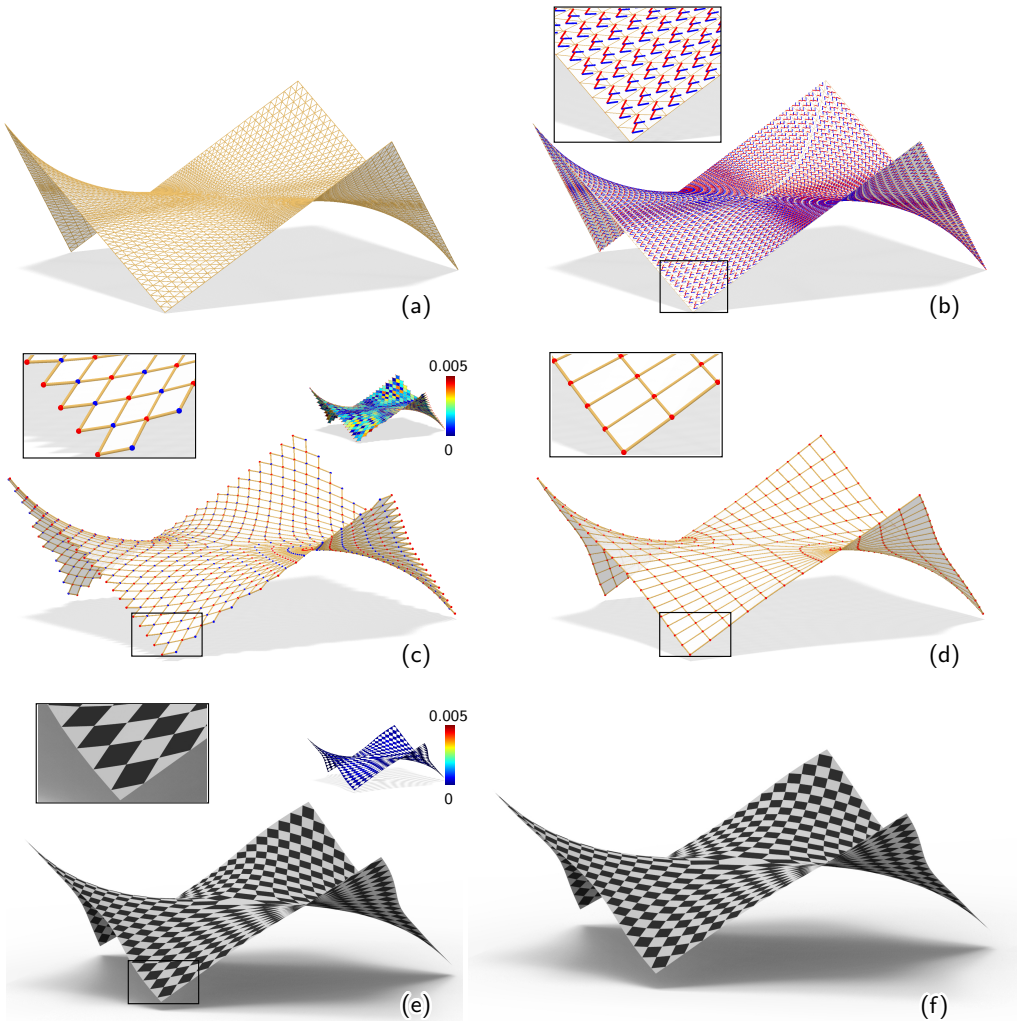


Figure 6: Re-meshing a surface, given as a triangle mesh (a), by a PQ mesh with constant angle 60°: (b) We define a pair of conjugate directions with angle 60° in each face of the input mesh. (c) We compute a quad mesh aligned with these directions. This mesh is colored with blue and red vertices. As the inset shows, its faces are not planar with high accuracy; planarity of a quad is measured as the distance of the two diagonals divided by their average length. (d) We take the mesh formed by the red vertices as control mesh and perform PQ optimization with constant angle 60° and proximity to the reference surface. (e) The result is shown with the checkerboard pattern of black parallelograms. As the inset shows, now also the white faces are planar with high accuracy. (f) shows another remeshing result with angle 75°.

α). There is a choice here in each point due to the symmetry of solutions with respect to principal directions. The selection has to be done in a consistent manner over the entire surface. This frame field is used as a guiding field for an initial quad mesh based on one of the available techniques from Geometry Processing. We use the implementation of mixed-integer quadrangulation (MIQ) of Bommes et al. (2009) in LIBIGL by Jacobson et al. (2018). In the resulting mesh M , we alternately color vertices, say as red and blue ones (Fig. 6, (c)) and take e.g. the red one as control mesh C (Fig. 6, (d)); note that its diagonals follow the edges of M . Now C is optimized for constant angle α between the diagonals, and the diagonal meshes D_1, D_2 for the PQ property. During this optimization, we ensure proximity to the given reference shape S as in Tang et al. (2014).

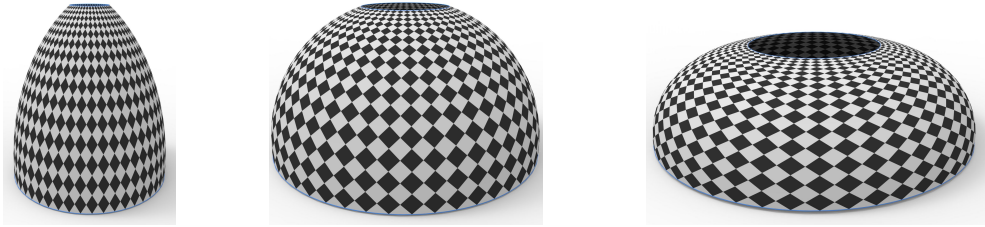


Figure 7: Rotationally symmetric CB patterns with planar white quads and similar black rhombuses. The constant angle is 60° (left), 90° (middle) and 120° (right). Due to the symmetry of these patterns with respect to the principal directions, these meshes represent surfaces with a constant ratio of principal curvatures. The constant angle α is related to the principal curvatures via $\tan^2(\alpha/2) = \kappa_1/\kappa_2$ and thus the middle surface represents part of a sphere.

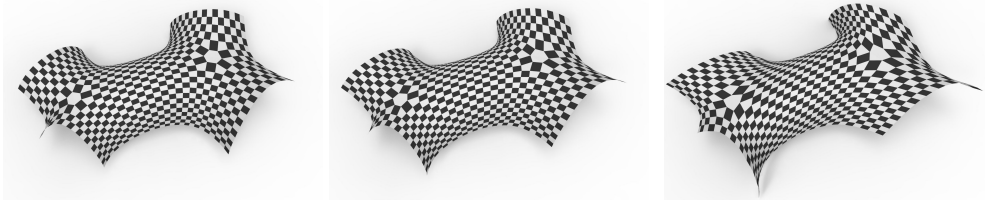


Figure 8: CB-patterns which are PQ meshes and exhibit a constant angle α : 90° (left), 75° (middle) and 60° (right).

Remark. The characteristic directions on a positively curved surface define a conjugate curve network which is symmetric with respect to the principal directions. It possesses a constant angle α only for surfaces with a constant positive ratio κ_1/κ_2 of principal curvatures. Principal symmetric curve networks have an appearance which may be more appealing than the network of principal curvature lines. A good example are rotational shapes, in which the latter are rather boring, but the former are much more interesting (see Fig. 18). Using results of Schling et al. (2018), one can easily construct quad meshes which are principal symmetric in a discrete sense. One has to ensure that each vertex and its four connected neighbors lie on a sphere. One could then even achieve a constant angle within our framework, by applying the sphere condition to both diagonal meshes D_1, D_2 and the constant angle on

the diagonals of the quads in the control mesh C . We do not further elaborate on this, but now turn to that limit case of principal symmetric meshes in which the mentioned spheres are planes.

Asymptotic nets with constant angle. When we are working with A-nets (discrete asymptotic parameterizations), we apply the A-net condition, namely planar vertex stars, to both diagonal meshes. Then, also the CB-pattern P is a discrete asymptotic parameterization, as its edges follow the corresponding directions in D_1, D_2 . However, for our applications, we do not need P at all. But we successfully apply the approach to the pair (D_1, D_2) , as we will see below.

Working with a mesh pair is beneficial if we want to express a constant angle or other constraints on the angle. We just have to realize this angle between corresponding edges of D_1, D_2 , i.e., the diagonals of the quads in the control mesh C . Since the asymptotic directions on a negatively curved surface ($K < 0$) form the angle α with $\tan^2(\alpha/2) = |\kappa_1/\kappa_2|$, a constant angle between asymptotic directions characterizes surfaces with a constant negative ratio of principal curvatures (see Fig. 9). Discrete versions have recently been studied by Jimenez et al. (2020), but our approach is simpler. Note that a constant right angle belongs to $\kappa_1 + \kappa_2 = 0$ which characterizes minimal surfaces. There is a rich literature on discrete minimal surfaces (see Bobenko and Suris (2008)), but the present approach based on diagonal meshes and orthogonal A-nets seems to be a new concept.

If we have aimed at an A-net with a constant angle, we actually got two of them: D_1 and D_2 . Only one is taken and then used as basis of asymptotic gridshells in the sense of Schling et al. (2018).

Rationalization of a negatively curved surface with an A-net is quite straightforward, and is initialized with a quad mesh that is aligned with the asymptotic directions of the reference surface. Of course, one cannot expect a constant angle in the mesh if the reference surface does not have a constant negative ratio of principal curvatures.

Remark. Surfaces with a relation between their principal curvatures are called Weingarten surfaces. Among other appealing properties (see Tellier (2020)), these surfaces possess advantages for paneling with curved panels. As they possess only a one-parameter family of different curvature elements, sufficiently small panels can be produced with a reduced number of molds. Roughly, N panels require only \sqrt{N} molds.

3 Optimization

In the following, we briefly discuss the mathematical formulation of the constraints and how they are solved within an optimization algorithm.

Angle constraints. Key constraints are those on angles, which are particularly easy to deal with. As shown in Fig. 11 left, the angle between the diagonals in each quad of the control mesh determines the inner angles of the black parallelogram.

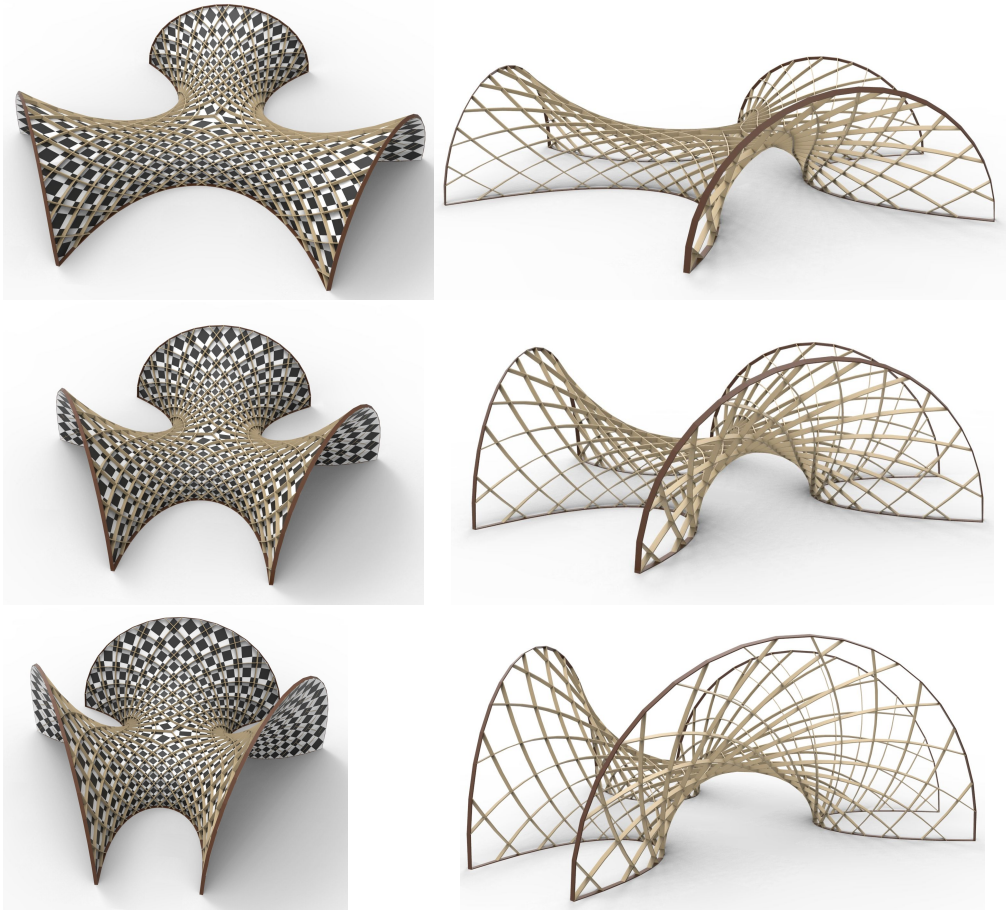


Figure 9: A-nets with constant angle 60° (top), 75° (middle) and 90° (bottom). They represent surfaces with constant principal curvature ratio $\kappa_1/\kappa_2 = C$ with $C = -1/3$ (top), $C = -0.58879$ (middle) and $C = -1$ (bottom). The latter surface is a minimal surface. Left: One diagonal mesh and the associated checkerboard pattern. Right: The diagonal mesh has been used as a basis for an asymptotic gridshell with constant node angle.

The constraint for a prescribed angle α is formulated as

$$c_{angle,i} = \frac{\mathbf{v}_{i2} - \mathbf{v}_{i0}}{\|\mathbf{v}_{i2} - \mathbf{v}_{i0}\|} \cdot \frac{\mathbf{v}_{i3} - \mathbf{v}_{i1}}{\|\mathbf{v}_{i3} - \mathbf{v}_{i1}\|} - \cos \alpha = 0, \quad (4)$$

where $\mathbf{v}_{i0}, \mathbf{v}_{i1}, \mathbf{v}_{i2}$, and \mathbf{v}_{i3} are the four vertices of face i . To simplify this formulation in the optimization, the diagonal lengths $\|\mathbf{v}_{i2} - \mathbf{v}_{i0}\|$ and $\|\mathbf{v}_{i3} - \mathbf{v}_{i1}\|$ can be taken from the previous iteration.

Black rhombuses. A black parallelogram becomes a rhombus when the control quad diagonals have the same length, i.e.

$$c_{length,i} = \|\mathbf{v}_{i2} - \mathbf{v}_{i0}\|^2 - \|\mathbf{v}_{i3} - \mathbf{v}_{i1}\|^2 = 0. \quad (5)$$

In the optimization, the above two constraints are formulated as energy terms $E_{angle} = \sum_{i=1}^{|F|} c_{angle,i}^2$ and $E_{length} = \sum_{i=1}^{|F|} c_{length,i}^2$.

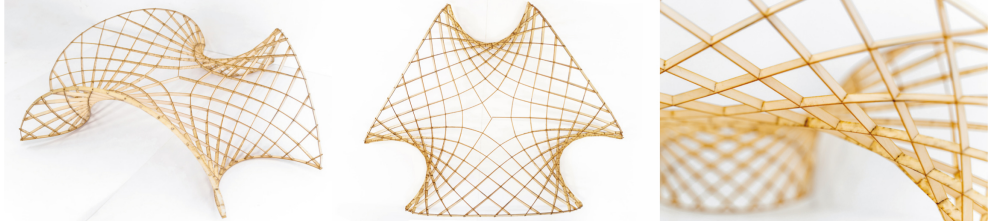


Figure 10: Timber model of the A-Net in Figure 9, bottom. The constant 90° angle allows for repetitive slot connections of minimum width.

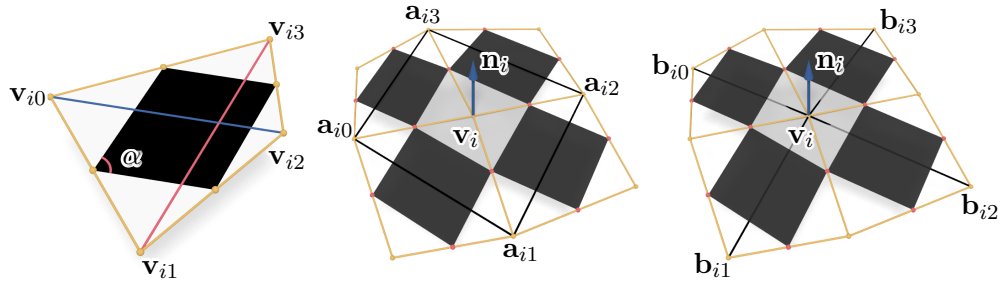


Figure 11: Geometric constraints for angles (left), planar white quads (middle) and A-nets (right).

PQ meshes. Since the black parallelograms are planar anyway, we have to enforce planarity of the white quads in a CB pattern. As shown in Fig. 11 middle, each vertex \mathbf{v}_i of the control mesh has a corresponding white quad which is a similar (with the scale ratio 1:2) to a quad in a diagonal mesh. This quad is formed by the neighbouring vertices \mathbf{a}_{i0} , \mathbf{a}_{i1} , \mathbf{a}_{i2} , and \mathbf{a}_{i3} of \mathbf{v}_i . To achieve its planarity, we introduce a normal vector \mathbf{n}_i of its plane as an additional variable and ensure that it is orthogonal to the edges of the quad $\mathbf{a}_{i0}\mathbf{a}_{i1}\mathbf{a}_{i2}\mathbf{a}_{i3}$ (see Tang et al. (2014)). To avoid that \mathbf{n}_i gets too small, we enforce it as a unit vector, leading to the term

$$E_{PQ} = \sum_{i=1}^{|V|} \sum_{j=0}^3 (\mathbf{n}_i \cdot (\mathbf{a}_{ij} - \mathbf{a}_{ik}))^2 + \sum_{i=1}^{|V|} (\mathbf{n}_i \cdot \mathbf{n}_i - 1)^2, \quad (6)$$

where the index $k \equiv j+1 \pmod{4}$.

A-nets. To optimize for a discrete asymptotic parameterization, the vertices of both diagonal meshes are required to have planar vertex stars. As illustrated in Fig. 11 right, let \mathbf{b}_{i0} , \mathbf{b}_{i1} , \mathbf{b}_{i2} , and \mathbf{b}_{i3} be the neighboring vertices of \mathbf{v}_i in the diagonal meshes. Then a planar vertex star is expressed via a normal \mathbf{n}_i as

$$E_{Anet} = \sum_{i=1}^{|V|} \sum_{j=0}^3 (\mathbf{n}_i \cdot (\mathbf{b}_{ij} - \mathbf{v}_i))^2 + \sum_{i=1}^{|V|} (\mathbf{n}_i \cdot \mathbf{n}_i - 1)^2. \quad (7)$$

Optimization. In addition to the terms resulting from constraints, we use a fairness term E_{fair} as described by Pottmann et al. (2007) and Jiang et al. (2020). The

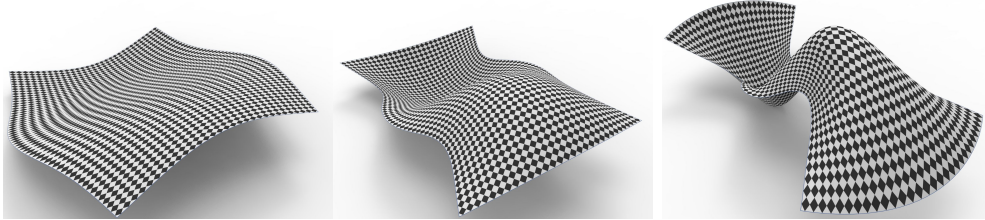


Figure 12: CB patterns with planar white quads and similar black rhombuses. The constant angle is 120° (left), 90° (middle) and 60°(right). Black quads are rhombuses and thus the surface in the middle is a discrete isothermic surface. The other two surfaces are discrete generalized isothermic surfaces whose mathematical study appears to be missing so far.

Fig.	V	F	#var	λ_1	λ_2	λ_3	λ_4	λ_5	#it	T[s]
6(e)	409	360	2454	1	0	1	0	0.1	10	0.3
6(f)	427	378	2562	1	0	1	0	0.1	10	0.3
7	800	750	4800	1	1	1	0	0.1	10	0.8
8	614	527	3684	1	0	1	0	0.1	10	0.4
9	1499	1440	8994	1	0	0	1	0.1	10	2.5
12	1860	1770	11160	1	1	1	0	0.01	10	1.5
13	787	720	4722	1	1	0	1	0.1	10	1.0
14	679	606	4074	1	1	0	1	0.1	10	0.8

Table 1: This table gives an overview of the size of optimization problems solved for various examples in this paper. We also provide the parameter settings and computation time in seconds.

final objective function is a weighted sum of the above energy terms,

$$E = \lambda_1 E_{angle} + \lambda_2 E_{length} + \lambda_3 E_{PQ} + \lambda_4 E_{Anet} + \lambda_5 E_{fair},$$

which can be optimized by a Levenberg-Marquardt method. Depending on the applications, we have different weight parameter settings.

- For a PQ mesh, we set $\lambda_4 = 0$.
- For A-nets, we set $\lambda_3 = 0$.
- When $\lambda_2 > 0$ (see Table 1), the black parallelograms are rhombi.

Examples. CB patterns from planar quads and with a fixed angle are shown in Figures 8, 7 and 12. In the latter two Figures, the black faces are rhombuses. This implies that all black faces are similar (scaled versions of each other). In Architectural Geometry, we have so far only seen PQ meshes with a right angle (circular and conical meshes), but there none of the faces has been a precise rectangle. In our CB patterns to $\alpha = \pi/2$, the black faces are exact rectangles. We can also achieve black squares, as in Fig. 7 and Fig. 12, middle. These are discrete isothermic surfaces. Figure 9 shows A-nets with constant angle α . These are discrete surfaces with constant negative ratio of principal curvatures,

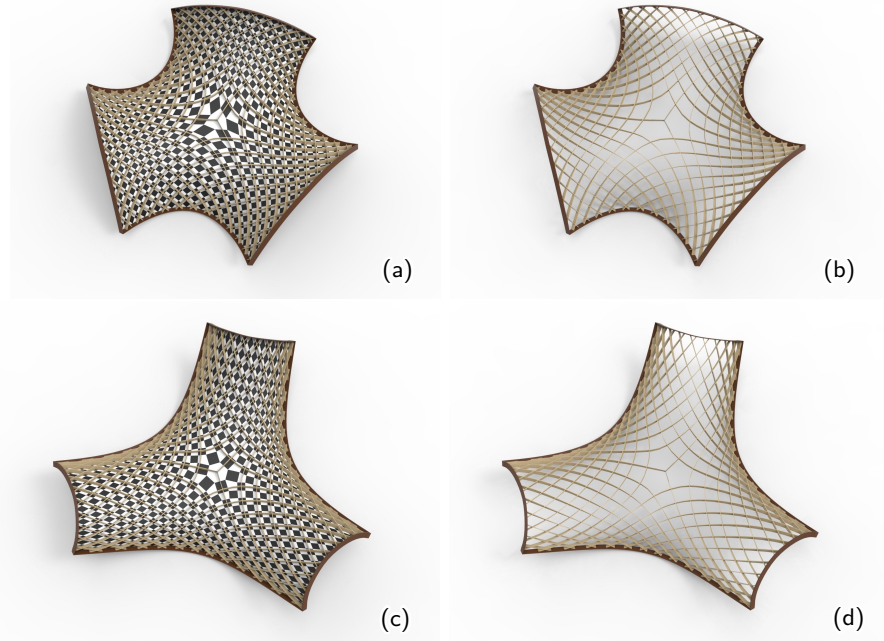


Figure 13: Angles as a design parameter. A-nets as checkerboard patterns (a,c) and asymptotic gridshells (b,d). For (a,b), the angle increases radially from the central singularity to the boundaries, in (c,d) it decreases.

$\kappa_1/\kappa_2 = -\tan^2(\alpha/2)$. In Fig. 13, we illustrate how the angle can be used as a design parameter.

4 Application in Architecture

This chapter will focus on the application of A-Nets in an architectural context. Specifically, we focus on *gridshells*, first developed by Frei Otto in the 1960s (Hennicke (1974)). Otto created doubly curved grids from an initially straight and flat grillage of slender timber laths. Most commonly, square or round profiles were used for this purpose, as they are able to bend and twist equally in all directions. Following the asymptotic networks allows us to use tall lamella profiles instead. The structural elements follow the paths of constant zero normal curvature and thus do not require any bending around their strong axis during the erection process.

This new construction method has enjoyed great popularity over the past years, with international applications in academic and commercial projects (Fig. 1). Learning from these built structures, we can identify potentials for design, fabrication, construction and load-bearing capacity.

4.1 Construction with constant node angles

The following series of prototypes and built structures documents a variety of constructive solutions for asymptotic gridshells. We focus specifically on the advantages of asymptotic nets with constant angles.

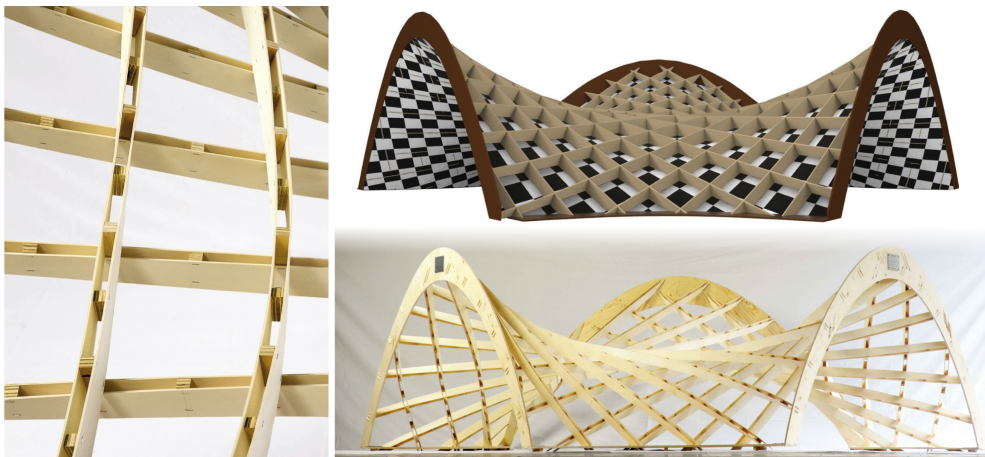


Figure 14: Diagonal mesh and associated checkerboard pattern of an A-Net with constant angle 90° on a Schwarz D minimal surface (top right). The Timber prototype is constructed with a slightly coarser network (bottom right). We introduce two parallel lamellas to allow for bending and post-coupling of the slender profiles. The two families of lamellas are constructed on separate levels and connected with square studs (left).

Timber prototype. The first timber prototype was built at approximately 4x4 m span (Fig. 14). The timber laths were assembled on two levels to allow for uninterrupted profiles of 60x4 mm polar plywood. Additionally, two parallel profiles were used for each edge in order to allow a smooth bending process during construction, but ensure high stiffness in the final structure. Once bent into the final position, the two timber lamellas are joined with shear blocks to act as one beam.

The two levels are connected with simple, square timber studs, which fix the constant 90° angle on bottom and top and act as rigid connection transferring bending and torsional moments. This stud could only be fitted if all elements were bent in their final geometry. Consequently, this prototype was erected spatially using a temporary framework and solid planar edge-beams as supports.

Steel gridshell. The first large scale Asymptotic Gridshell (Fig. 1, top) was constructed from straight 1.5 x 100 mm steel strips. The metal strips were first slotted together by hand into flat segments, creating a scissor joint at each intersection that allowed to deform the whole segment into its design shape. The constant 90° angles offered a control-mechanism of the design geometry during the bottom-up erection process, allowing to deform and fix the final shape of the double-curved segments without the need for form-work. Again two parallel lamellas were used which created a central void at each intersection allowing a simple connection with a single bolt and repetitive star-shaped washers (Fig. 15 d).

Asymptotic Urban Roof. Current research is looking at potentials for large-scale steel and glass construction to combine the structural benefits of double curvature with repetitive and simplified fabrication of joints, beams and panels. The design of an urban metro station (Fig. 16) is based on an optimized A-net with constant

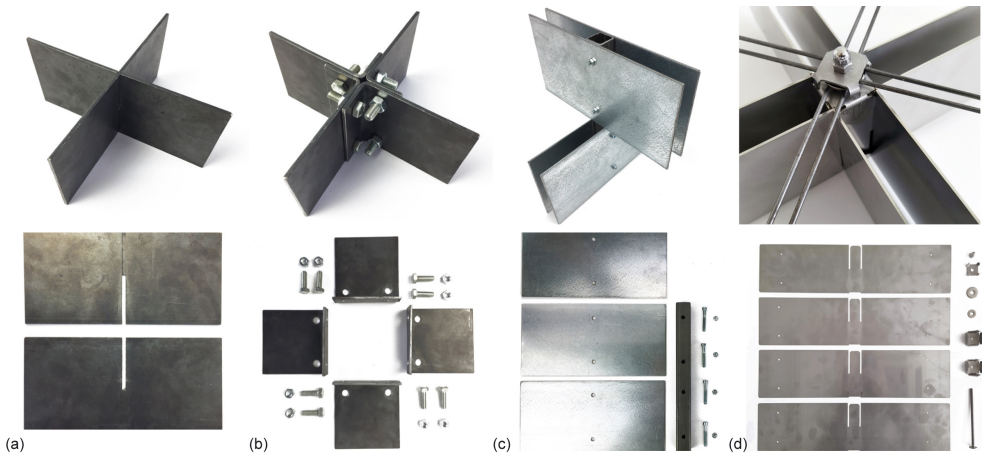


Figure 15: Development of orthogonal steel joints, looking at (a) a simple slotted and welded connection (b) segmented, reciprocal lamellas, (c) double lamellas on two levels connected by a square pipe and (d) a double slotted connection with star-shaped connectors. The latter was used for the construction of the Asymptotic Gridshell.

angle 60° (Fig. 9). In this scenario, the repetitive joints can be prefabricated and assembled on site with straight steel segments of varying length. The facade is triangulated through secondary profiles that brace the structure and frame the planar glass panels.

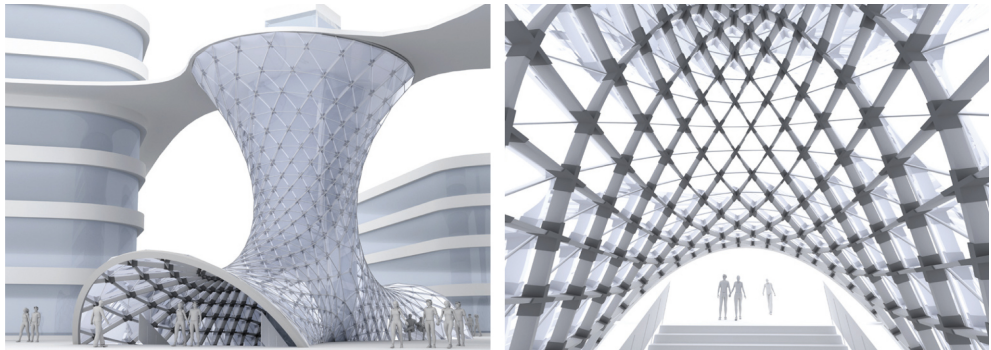


Figure 16: Design of an urban metro station using the optimized A-net with constant angle 60° from Figure 9.

4.2 Angles as a design parameter

While constant node angles provide great benefits for the fabrication of asymptotic gridshells, they also limit their design freedom. In the following, we will introduce two further projects which deliberately use varying node angles, as means to follow the structural or transformational behaviour.

Asymptotic Canopy. The first permanent Asymptotic Gridshell was completed in December 2019 for the Intergroup Hotel in Ingolstadt (Schikore et al. (2019)) (Fig. 1, bottom and Fig. 17, right). The surface was designed with a gradual shift

of intersection angles from almost 90° at the top to roughly 60° at the bottom, thus creating a structurally informed topology that would allow for a smooth load-transfer towards the supports. Each of the four symmetric segments was first assembled flat and then pulled upside down to create the funicular design (Fig. 17, left). The stainless steel structure was built from single 2.5×100 mm lamellas (similar to Fig. 15 a) with slots of varying width for each intersection. These individual slots set the correct angle at each joint and thus aided to define the design geometry before being welded in their position.



Figure 17: Asymptotic Canopy for the Intergroup Hotel in Ingolstadt. The grid is designed with a transition from 90 to approximately 60 node angles, thus allowing for a bespoke shape and a directed load-path. Each segment prefabricated hanging upside down, to form the design geometry.

Asymptotic Umbrella. The Asymptotic Umbrella (Fig. 18) is an ongoing research project to be exhibited at the AAG in Paris. It utilizes the predictable deformation behaviour of lamella-grids to create a transformable structure. The lamellas are constructed from continuous, rectangular, hollow GRP sections. All joints are hinged in order to accommodate the transformation from cylindrical to funnel shape. The design follows similar geometric principles as our studies in Figure 13, with node angles decreasing toward the top for a closed, conical configuration, and increasing in the unfolded funnel shape. The umbrella mechanism is actuated by vertical cables, which gradually open these angles, thus causing the grid to change shape, open up and move downwards. During this process, the radius at the base remains constant.

4.3 Conclusion and future research

We have introduced a new concept for the design of constrained quad meshes which exploits the geometry of the two diagonal meshes of a control mesh. This turns out to be particularly useful for the control of node angles and shape properties of quads in the mesh and the associated checkerboard pattern arising through mid-edge subdivision. In particular, we applied this method to the design of asymptotic gridshells with constant or controlled intersection angles. We discussed related developments for the construction in timber and steel, and showed future applications for large scale and transformable structures.



Figure 18: The Asymptotic Umbrella is a transformable structure. It is actuated by vertical cables which gradually open the angles in the upper part of the grid, causing the umbrella to unfold.

According to Jiang et al. (2020), the diagonal mesh approach is also a simple tool for modeling developable surfaces, especially for applications where one needs to deform them isometrically, i.e., by pure bending. Our ongoing research extends this method to address the inclusion of material behaviour for architectural paneling solutions. Moreover, we aim to include structural behaviour into the design process, to inform the shape and topology of lamella gridshells. The geometry of transformable structures associated with asymptotic gridshells and their behavior during the erection process is another rewarding topic for future research in both theory and practice.

Acknowledgements

This work was supported by KAUST baseline funding, the University of Hong Kong (HKU) Seed Fund and the Technical University in Munich (TUM) Architectural Research Incubator (ARI). We thank Wesley She, Muye Ma and Denis Hitrec for their commitment in producing timber models, visualizations and steel prototypes to test and verify our findings. The Asymptotic Gridshell and Asymptotic Canopy were constructed with and by the Erhard Brandl Steel Manufacturer in Eitensheim (www.brandl-eitensheim.de). We are very grateful for their dedication and professional know-how.

References

- Adiels, E., C. Brandt-Olsen, J. Isaksson, I. Näslund, K.-G. Olsson, E. Poulsen, and C. J. K. Williams (2019). The design, fabrication and assembly of an asymptotic timber gridshell. In C. Lázaro, K.-U. Bletzinger, and E. Oñate (Eds.), *FORM and FORCE 2019*, pp. 717–724. Barcelona: International Centre for Numerical Methods in Engineering (CIMNE).
- Bobenko, A. I., W. K. Schief, Y. B. Suris, and J. Techter (2016). On a discretization of confocal quadrics. i. an integrable systems approach. *Journal of Integrable Systems* 1(1).
- Bobenko, A. I. and Y. B. Suris (2008). *Discrete differential geometry. Integrable structure*, Volume 98 of *Graduate Studies in Mathematics*. American Mathematical Society, Providence, RI.
- Bommes, D., H. Zimmer, and L. Kobbelt (2009, July). Mixed-integer quadrangulation. *ACM Trans. Graph.* 28(3), 77:1–77:10.
- Hennicke, J. (1974). IL10 Gitterschalen. Sonderforschungsbereich weitgespannte Flächentragwerke. Stuttgart, Institut für leichte Flächentragwerke.
- Jacobson, A., D. Panozzo, et al. (2018). libigl: A simple C++ geometry processing library. <https://libigl.github.io/>.
- Jiang, C., C.-H. Peng, P. Wonka, and H. Pottmann (2019). Checkerboard patterns with black rectangles. *ACM Trans. Graphics* 38(6), 171:1–171:13.
- Jiang, C., C. Wang, F. Rist, J. Wallner, and H. Pottmann (2020). Quad-mesh based isometric mappings and developable surfaces. *ACM Trans. Graphics* 39(4), 128:1–128:13.
- Jimenez, M. R., C. Müller, and H. Pottmann (2020). Discretizations of surfaces with constant ratio of principal curvatures. *Discrete & Computational Geometry* 63, 670–704.
- Kenyon, R. (2002, Nov). The Laplacian and Dirac operators on critical planar graphs. *Inventiones mathematicae* 150(2), 409–439.
- Liu, Y., H. Pottmann, J. Wallner, Y.-L. Yang, and W. Wang (2006). Geometric modeling with conical meshes and developable surfaces. *ACM Trans. Graphics* 25(3), 681–689.
- Maxwell, I. (2019). Supersuccah: Sculpture by the Sea, Bondi, 2019. www.sculpturebythesea.com, accessed: 25.03.2020.
- Pottmann, H., M. Eigensatz, A. Vaxman, and J. Wallner (2015). Architectural geometry. *Computers and Graphics* 47, 145–164.

- Pottmann, H., Y. Liu, J. Wallner, A. Bobenko, and W. Wang (2007). Geometry of multi-layer freeform structures for architecture. *ACM Trans. Graphics* 26(3), 65:1–65:11.
- Rabinovich, M., T. Hoffmann, and O. Sorkine-Hornung (2018). Discrete geodesic nets for modeling developable surfaces. *ACM Trans. Graph.* 37(2), 16:1–16:17.
- Schikore, J., A. M. Bauer, R. Barthel, and K.-U. Bletzinger (2019). Large torsion on elastic lamella grid structures. In C. Lázaro, K.-U. Bletzinger, and E. Oñate (Eds.), *FORM and FORCE 2019*, pp. 788–795. Barcelona: International Centre for Numerical Methods in Engineering (CIMNE).
- Schling, E. (2018). *Repetitive Structures*. Ph. D. thesis, Chair of Structural Design, Technical University of Munich, DOI: 10.14459/2018md1449869.
- Schling, E., D. Hitrec, J. Schikore, and R. Barthel (2017). Design and construction of the asymptotic pavilion. In K.-U. Bletzinger, E. Oñate, and B. Kröplin (Eds.), *VIII International Conference on Textile Composites and Inflatable Structures*, pp. 178–189. International Center for Numerical Methods in Engineering (CIMNE).
- Schling, E., M. Kilian, H. Wang, D. Schikore, and H. Pottmann (2018). Design and construction of curved support structures with repetitive parameters. In L. H. et al. (Ed.), *Adv. in Architectural Geometry*, pp. 140–165. Klein Publ. Ltd.
- Schling, E. and J. Schikore (2020). Asymptotic Canopy: Intergroup Hotel Ingolstadt. www.eikeschling.com, accessed: 25.03.2020.
- Shih, S.-G., H. Chen, C. Hsu, K. Yen, and C. Lee (2019). Element-based lifecycle information modelling for curved building skins. Economic Forum, Taiwan.
- Tang, C., X. Sun, A. Gomes, J. Wallner, and H. Pottmann (2014). Form-finding with polyhedral meshes made simple. *ACM Trans. Graph.* 33(4), 70:1–70:9.
- Techter, J. (2020). *Discrete confocal quadrics and checkerboard incircular nets*. Ph. D. thesis, TU Berlin.
- Tellier, X. (2020). *Morphogenesis of curved structural envelopes under fabrication constraints*. Ph. D. thesis, Univ. Paris-Est.